Manufacturing Tolerances: Estimation and Prediction of Cogging Torque Influenced by Magnetization Faults

I. Coenen, M. van der Giet, and K. Hameyer

Institute of Electrical Machines, RWTH Aachen University, Aachen 52056, Germany

Permanent-magnet excited synchronous motor servo drives are increasingly employed in industrial applications. During mass production, deviations from the ideal machine occur. Thereby, parasitic effects such as cogging torque and torque ripple are influenced in particular. For permanent-magnet excited machines, the magnet's quality is important. There are many possible failure configurations requiring the study of their influence on the machine's behavior. In this paper, an approach for the estimation of cogging torque considering magnetization faults is presented. This approach is applied to determine crucial configurations of permanent-magnet faults. The intent is to evaluate the influence of the faulty magnetic materials with its asymmetries on the later produced machine. In the process, analytical and numerical methods are combined whereby finally a small computational effort with accurate results is achieved.

Index Terms—**Cogging torque, electrical machine, estimation of manufacturing fault tolerance, magnetization fault, permanent-magnet motor, servo-drive.**

I. Introduction

ELECTRICAL machines offer a lot of advantages in terms of efficiency and dynamic performance. Therefore, their application as servo drives is increasing and they are manufactured in significant quantity. However, electrical machines present parasitic effects such as torque ripple, losses or acoustic noise which need to be evaluated. Material dependant failures, geometrical or shape deviations may occur during the manufacturing process leading to a non-ideal machine. These deviations have a strong influence on the afore mentioned parasitic effects.

A relevant parasitic effect occurring in case of permanent-magnet excited machines is cogging torque. It is strongly influenced by manufacturing tolerances [1]. In particular, tolerances in the magnetic material present a significant impact. To prove every permanent magnet before inserting it into the machine would involve a large effort and is usually not performed during mass production. For a certain machine, it is helpful to find out the worst cases to know the most crucial influences that could appear. It is later on possible to take measures to avoid these worst cases. For instance, a robust design approach can be applied [2]. Thereby, the distribution of the magnetic flux in the rotor is altered by applying changes to the machine's design to achieve a minimization of cogging torque. This is done with respect to manufacturing variations to obtain a robust design.

Performing the study of possible failure configurations by numerical methods such as finite element analysis (FEA) would imply a high computational effort. Hence, a method predicting the cogging torque is required which involves less effort and delivers accurate results. The majority of the multiple existing analytical approaches [3], [4] are applied to electrical machines with surface mounted permanent magnets (SPM). But most of them are either complex or require simplifications. Furthermore, the existing approaches are not extended to consider magnetization faults. In this study, machines with interior mounted permanent magnets (IPM) are investigated. The prediction of cogging torque for this type of machine is more difficult compared to SPM due to the saturation appearing in the iron parts linking magnets and air gap. In [5] an analytical approach is given. But it is performed applying simplifications. For instance, the flux distribution in the slots' region is simplified. In addition, an extension of the method would be required for consideration of asymmetries in the magnetic material.

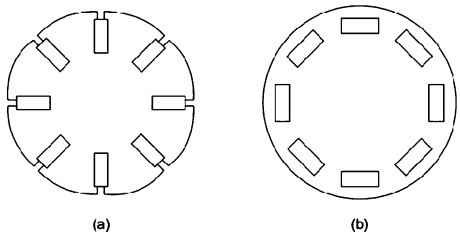

Fig. 1. Rotor constructions: (a) Spoke configuration. (b) Buried magnets.

In the following, an approach is presented combining minor computational effort and accurate results with due regard to magnetization tolerances.

II. Studied Machines

In this work, there are two permanent-magnet excited synchronous machines investigated. They both present interior permanent magnets. IPM1 contains six stator slots and four pole pairs with a spoke configuration of the magnets. IPM2 also presents four pole pairs, but 18 stator slots and buried magnets. The data of IPM1 and IPM2 is collected in Table I. The two different rotor constructions are shown in Fig. 1.

III. Cogging Torque

For permanent-magnet excited synchronous machines cogging torque is an undesired effect which occurs due to the interaction between the stator slots and the rotor magnets. Here, the air gap length varies periodically because of the stator slotting which leads to an alternating permeance at the air gap. The thereby evoked periodically oscillation of the magnetic energy leads to a pulsating torque, even at no-load operation. Cogging torque is undesired because rotational oscillations of the drive

Manuscript received September 20, 2011; revised November 08, 2011; accepted November 23, 2011. Date of publication December 07, 2011; date of current version April 25, 2012. Corresponding author: I. Coenen (e-mail: isabel.coenen@iem.rwth-aachen.de).

Digital Object Identifier 10.1109/TMAG.2011.2178252

TABLE I
STUDIED MACHINES

	IPM1	IPM2
Number of pole pairs p	4	4
Number of stator slots N	6	18
Rotor construction	Spoke configuration	Buried magnets

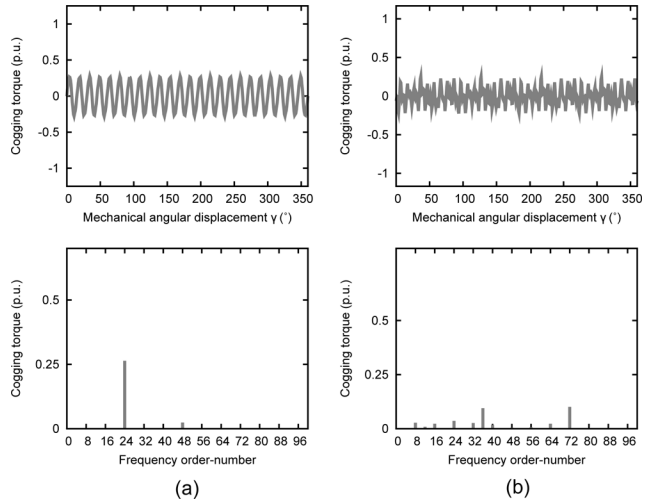

Fig. 2. Time function of cogging torque for one rotor revolution and cogging torque spectrum for (a) IPM1and (b) IPM2.

train are excited. To reduce this effect, there are various approaches for cogging torque minimization [6], [7].

Fig. 2 shows the cogging torque time function of the two analyzed machines for one rotor revolution. This is calculated applying a time-stepping FEA for no-load operation. The interesting value is the peak-to-peak cogging torque ΔT. The corresponding discrete Fourier transform (DFT) yields the spectrum as also presented in Fig. 2. The main harmonic order n of the cogging torque is obtained from the least common multiple (LCM) of pole and slot number [8]:

$$n = \mathrm{LCM}(2p, N) \tag{1}$$

which is 24 for IPM1 and 72 for IPM2.

For IPM2 the spectrum also shows lower frequency orders than the main order 72. Those appear due to the stator geometry, e.g., notches on the circumference of the stator.

IV. MAGNETIZATION FAULTS

For permanent-magnet excited machines the quality of the permanent-magnet material is an important aspect. Possible deviations concerned here are the magnitude of the remanence flux-density B_R and the angle β of the direction of magnetization. These two tolerances are illustrated in Fig. 3.

Concerning cogging torque, it has been shown that a variation from the remanence flux-density B_R preponderates compared to variations in the magnetization direction [9]. This fault will be investigated in the following.

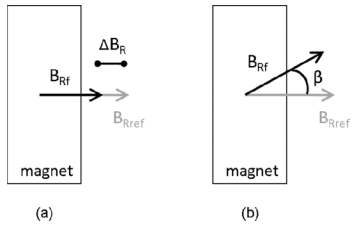

Fig. 3. Magnetization tolerances: (a) magnitude of B_R, (b) magnetization direction β.

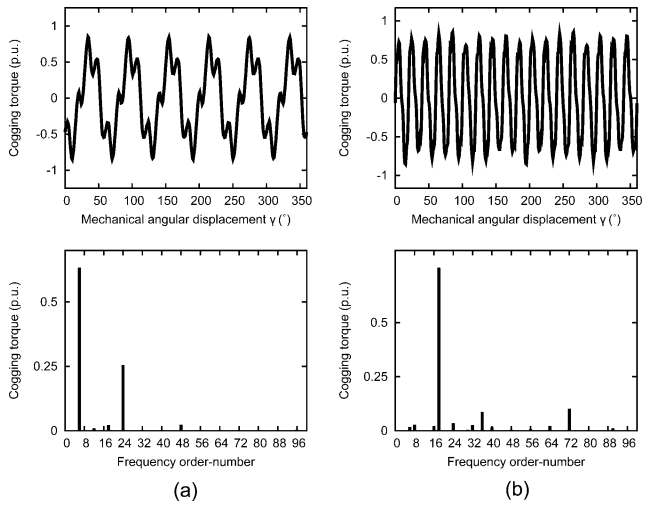

Fig. 4. Magnetization fault: Time function of cogging torque for one rotor revolution and cogging torque spectrum for (a) IPM1 and (b) IPM2.

During the manufacturing process, the permanent magnets are usually inserted into the rotor construction without proving their quality. It is not known, if there are magnets which are affected by deviations. The only available information is the possible deviation specified in the magnet's data sheet. The following study is based on realistic tolerance ranges.

A. Influence on Cogging Torque

Cogging torque is especially sensitive about magnetization faults [1], as their occurrence lead to an asymmetrical distribution of the air gap flux-density and in consequence to additional content of the cogging torque spectrum.

Fig. 4 shows the course of cogging torque and its spectrum for IPM1 and IPM2 resulting from faulty permanent magnets. Here, in each case one magnet presents a decrease by 10% of magnitude of remanence flux-density compared to its reference value.

The results from Fig. 4 differ from the results of the faultless case shown in Fig. 2. The course of cogging torque shows an increase of peak-to-peak cogging torque of about the triple value. New harmonic orders appear in the spectrum, which are a multiple of the slot number N. Thereby, the amplitude of these new orders depends on which and how many magnets are affected and on the intensity of the defect.

To know the most crucial influences that could appear, the worst cases are to be defined. For a machine with p pole pairs,

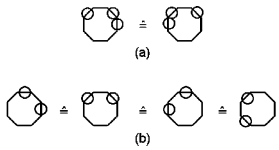

Fig. 5. (a) Mirror-symmetric configurations and (b) rotationally-symmetric configurations.

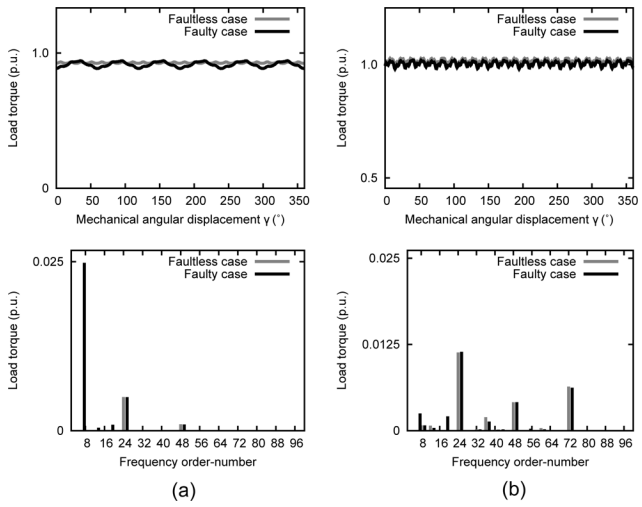

Fig. 6. Time function of load torque for one rotor revolution and load torque spectrum (without steady component) for (a) IPM1 and (b) IPM2.

the number of possible configurations is 2^{2p}. These can be reduced by symmetry conditions to a certain number of relevant configurations to be studied. Design-of-Experiments [10] is applied and rotationally- and mirror-symmetric configurations are exploited to reach a minimum of configurations to study.

The analyzed machines both present four pole pairs and therefore $2^8 = 256$ possible configurations which can be reduced to 18 relevant ones. Thereby, all configurations which are mirror- or rotationally-symmetric towards each other are excluded as they present the same course and amount of cogging torque considering one rotor revolution. Examples of symmetric configurations are shown in Fig. 5. One octagon represents the eight magnets of the machine and a defective one is tagged with a circle.

With higher pole pair numbers p, the number of possible configurations increases and so does the effort for cogging torque computation.

B. Influence on Load Torque

The indicated effects of magnetization faults also appear under load operation. For IPM1 and IPM2, the load torque is calculated with FEA and the resulting time function and DFT spectrum are plotted in Fig. 6. This is done for the faultless case as well as for the faulty case with one defective permanent magnet. It shows that the torque ripple under load operation is also influenced by magnetization faults. Furthermore, the new harmonic orders which are a multiple of N also appear in the load torque spectrum.

V. Estimation Technique

The specific problem of this work is to find crucial configurations of magnetization faults. The larger the number of poles, the larger is the number of configurations to investigate. Therefore, a fast method for the prediction of cogging torque is required. Here, an approach combining analytical and numerical methods is applied. For the numerical study, the number of required time-stepping FEA simulations is reduced to two. In the following this approach is named IEM (Institute of Electrical Machines) approach.

The basis for the cogging torque calculation is the Maxwell Stress Tensor (MST) [11]:

$$T(\gamma) = \frac{l_Z}{\mu_0} R^2 \int_0^{2\pi} B_r(\gamma,\alpha) \cdot B_t(\gamma,\alpha) \cdot d\alpha. \tag{2}$$

Here, R is the air gap radius, l_Z the length of the machine, α the relative position at the air gap and γ the relative mechanical angular displacement between stator and rotor. $B_r(\gamma,\alpha)$ and $B_t(\gamma,\alpha)$ are the radial and tangential flux-densities at the air gap of the machine.

The MST is employed when the torque is calculated with FEA and for this approach it also builds the basis for the analytical computation.

In case of magnetization faults, the radial and tangential flux-density functions $B_r(\gamma,\alpha)$ and $B_t(\gamma,\alpha)$ will differ from the faultless case with $B_{r0}(\gamma,\alpha)$ and $B_{t0}(\gamma,\alpha)$. They can be described by

$$B_r(\gamma,\alpha) = B_{r0}(\gamma,\alpha) + \sum_{i=1}^{2p} b_i \cdot \Delta B_{ri}(\gamma,\alpha), \tag{3}$$

$$B_t(\gamma,\alpha) = B_{t0}(\gamma,\alpha) + \sum_{i=1}^{2p} b_i \cdot \Delta B_{ti}(\gamma,\alpha). \tag{4}$$

Thereby, ΔB is defined to be the difference between the faulty function $B_f(\gamma,\alpha)$ and the faultless function $B_0(\gamma,\alpha)$. The vector b indicates which magnet is defective.

Fig. 7 shows $\Delta B_r(\gamma,\alpha)$ and $\Delta B_t(\gamma,\alpha)$ in case of one defective magnet at $\alpha = 210°$ compared to the faultless $B_{r0}(\gamma,\alpha)$ respectively $B_{t0}(\gamma,\alpha)$ for one rotor position γ. The defective magnet has a remanence flux-density B_R reduced by 10%. Comparing $B_r(\gamma,\alpha)$ of the two different machines, IPM1 shows a sinusoidal behavior. The reason behind is the geometry of stator and rotor of this machine which are shaped in such a way that a sinusoidal behavior of the air gap flux-density is achieved. This is not the case for IPM2 as Fig. 7 shows.

For the presented approach, two underlying FEA calculations are needed: the faultless case and the case where one magnet is defective. In each case the air gap is being sampled to calculate the discrete flux-density functions for every α and γ.

With $B_{r0}(\gamma,\alpha)$ and $B_{t0}(\gamma,\alpha)$ from the faultless case and $\Delta B_r(\gamma,\alpha)$ and $\Delta B_t(\gamma,\alpha)$ from the case where one magnet is defective, $B_r(\gamma,\alpha)$ and $B_t(\gamma,\alpha)$ can be evaluated for each possible configuration. Thereby, the vector b is important as it indicates which magnet is defective and therefore at which position the fault appears.

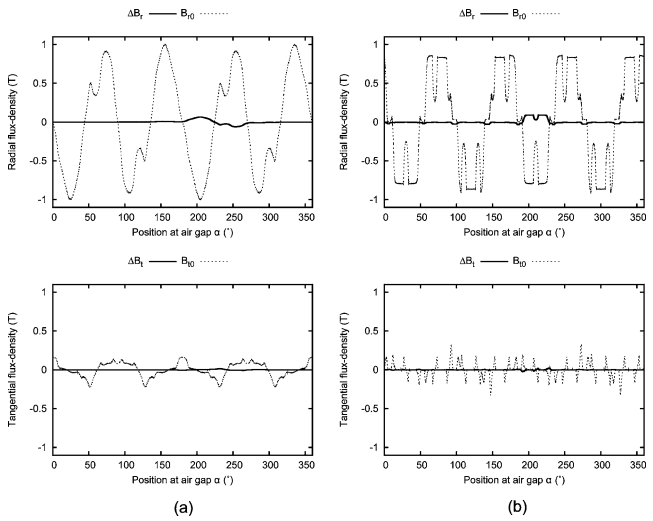

Fig. 7. Radial and tangential flux-density component for one defective magnet versus air gap angle α for (a) IPM1 and (b) IPM2.

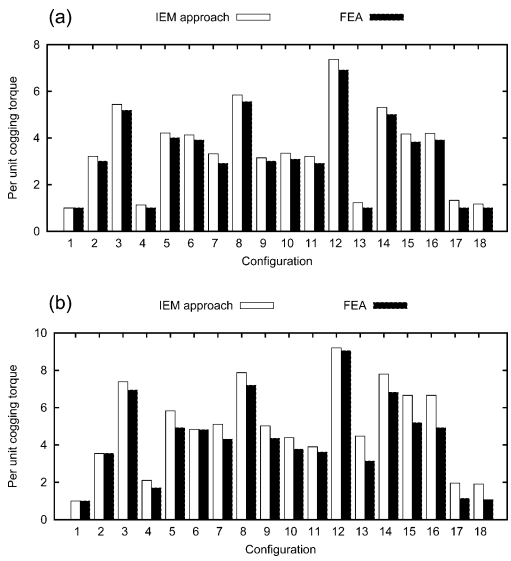

Fig. 8. Cogging torque distribution for relevant permanent-magnet configurations ($\Delta \mathrm{B_R} = -10\%$) for (a) IPM1 and (b) IPM2.

Finally, with (2), (3), and (4) the cogging torque $T(\gamma)$ and its spectrum $T(n)$ can now be evaluated for every possible configuration.

A computer program realizes this algorithm, which reads in the flux-density functions and calculates $T(\gamma)$ iterating over b.

A. Crucial Configurations

To find the worst case configurations of magnetization faults concerning cogging torque, the latter is calculated for the 18 relevant configurations.

The results for a variation of $\Delta B_R = -10\%$ are shown in Fig. 8. For verification of the IEM approach, the results are compared to the corresponding FEA results and the study is performed for both machines. In either case, the values of IEM approach and FEA differ, but the qualitative distribution is the same. On average, the results differ around 10% for IPM1 and 20% for IPM2. The achieved results for IPM1 are more accurate due to the sinusoidal course of the machine's air gap flux-density which can be established more precise. But for both machines the FEA and IEM approach results show the same qualitative distribution and present configuration 12 to have the most crucial influence on cogging torque.

It can be stated that the applied approach is accurate enough to find the worst configurations of magnetization errors. At this, there is an enormous gain of time compared to FEA: half a minute compared to four hours, in each case computing the cogging torque over one revolution for one failure configuration. Finally, this approach has a large potential of saving effort for machines with large pole numbers.

B. Stochastic Analysis

In [12] the influence of varying qualities of the permanent magnet on the cogging torque has been shown. The results have been generated applying a stochastic analysis where the different qualities and tolerances are modeled by different probability distributions. The aim is to verify the allowed and therefore acceptable tolerance ranges respecting a particular quality. This procedure requires a large number of test configurations to evaluate and compare the outcome cogging torque distributions. This presents a high computational effort when performing this analysis with FEA calculations.

To allow a time-saving realization, the same approach as discussed above can be applied here. A scaling factor s is introduced to study different percental variances of B_R.

$$\Delta B = s \cdot (B_{f\_-10} - B_0)\,. \tag{5}$$

The factor s relates any variance to the variance of -10%. It is determined by comparing the flux-density functions for different deviations ΔB_R. There are only the results of two FEA simulations required to calculate the torque $T(\gamma)$.

As an example, the remanence flux-density B_R is assumed to be normally distributed following the probability density function

$$f(x) = \frac{1}{\sigma\sqrt{2\pi}} \cdot \exp\left(-\frac{1}{2}\left(\frac{x-\mu}{\sigma}\right)^2\right). \tag{6}$$

The variable x represents B_R. The expected value μ is defined to be the reference value of B_R and a tolerance range Δx of $\pm 10\%$ is considered, which is equal to three times the standard deviation σ. For IPM2, there are 30 random failure configurations created and their cogging torque is calculated with the presented approach. The resulting peak-to-peak values are divided into five intervals I to V, whereby I is the interval with the lowest and V the interval with the highest values of cogging torque. Fig. 9 shows the resulting frequency distribution in comparison to FEA results.

Table II presents the per unit cogging torque for the applied intervals. Thereby, the cogging torque of each method is related to the corresponding reference cogging torque of the faultless machines. As determined in Fig. 8, the cogging torque calculated with the presented approach is about 20% higher compared

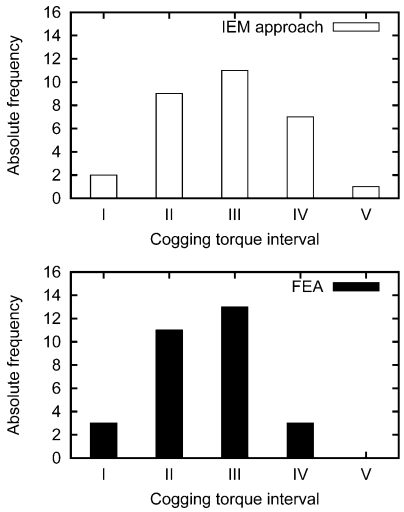

Fig. 9. Frequency distribution for normally distributed B_R.

TABLE II
COGGING TORQUE INTERVALS

Interval	IEM approach p.u. cogging torque	FEA p.u. cogging torque
I	2 - 3	1.6 - 2.6
II	3 - 4	2.6 - 3.6
III	4 - 5	3.6 - 4.6
IV	5 - 6	4.6 - 5.6
V	6 - 4	5.6 - 6.6

to FEA. Therefore, the corresponding initial value of interval I is set to be 20% higher than the value for the FEA results.

The two resulting distributions are qualitatively similar to each other. The results achieved by the presented approach show higher variance of distribution. It can be concluded that the presented approach can be used to evaluate statistical coherences. In addition, it can be stated that the chosen approach is very efficient when compared to FEA.

VI. CONCLUSION

In this study, an approach for the prediction of cogging torque with regard to magnetization faults is presented. Analytical and numerical methods are combined leading to a minor computational effort and qualitatively precise results. This approach can quickly be employed to study permanent-magnet machines by analyzing the worst case permanent-magnet configuration. The method is successfully applied for machines with interior mounted magnets. Furthermore, this method is extended in such a way that a stochastic analysis can be performed. Here, a large number of required calculations can be realized. This allows investigating different qualities of the permanent magnets. Finally, with the presented method it is possible to evaluate the influence of the magnetic material and its tolerances on the later produced machine. This information is valuable for the mass production of the machine and its subsequent application as a servo drive. Depending on the application, there are certain requirements on cogging torque. Employing this investigation, it is possible to prove if these can be achieved with respect to the allowed tolerance ranges. If not, either a robust design of the machine or an adjustment of the allowed tolerances is to be considered.

REFERENCES

[1] L. Gasparin, A. Cernigoj, S. Markic, and R. Fiser, "Additional cogging torque components in permanent-magnet motors due to manufacturing imperfections," *IEEE Trans. Magn.*, vol. 45, no. 3, pp. 1210–1213, Mar. 2009.

[2] M. Islam, R. Islam, T. Sebastian, A. Chandy, and S. Ozsoylu, "Cogging torque minimization in PM motors using robust design approach," in *IEEE Energy Conversion Congress and Exposition (ECCE)*, Atlanta, GA, Nov. 2010.

[3] L. Zhu, S. Z. Jiang, Z. Q. Zhu, and C. C. Chan, "Comparison of alternate analytical models for predicting cogging torque in surface-mounted permanent magnet machines," in *IEEE Vehicle Power and Propulsion Conf.*, Harbin, China, Sep. 2008.

[4] L. Wu., Z. Zhu, D. Staton, M. Popescu, and D. Hawkins, "Comparison of analytical models for predicting cogging torque in surface-mounted PM machines," in *XIX Int. Conf. Electrical Machines (ICEM)*, Sep. 2010.

[5] G. Kang and J. J. Hur, "Analytical prediction and reduction of the cogging torque in interior permanent magnet motor," in *IEEE Int. Conf. Electric Machines and Drives*, Dec. 2005.

[6] A. Q.-I. Deng, B. S. Hong, and C. F. Xiao, "Influence of design parameters on cogging torque in directly driven permanent magnet synchronous wind generators," in *Int. Conf. Electrical Machines and Systems (ICEMS)*, Tokyo, Japan, Nov. 2009.

[7] D. Wang, X. Wang, Y. Yang, and R. Zhang, "Optimization of magnetic pole shifting to reduce cogging torque in solid-rotor permanent-magnet synchronous motors," *IEEE Trans. Magn.*, vol. 46, no. 5, pp. 1228–1234, May 2010.

[8] C. Schlensok, M. Kurzidem, and K. Hameyer, "Novel method for fast analysis of cogging-torque harmonics in permanent-magnet synchronous-machines," in *12th Biennial IEEE Conf. Electromagnetic Field Computation (CEFC)*, Florida, Jun. 2006.

[9] C. Schlensok and K. Hameyer, "Analysis of cogging torque harmonics due to manufacturing tolerances in permanent magnet synchronous machines," in *7th Int. Symp. Electric and Magnetic Fields (EMF)*, France, Jun. 2006.

[10] J. Antony, *Design of Experiments for Engineers and Scientists*. London, U.K.: Butterworth-Heinemann, 2003.

[11] F. Henrotte, "Handbook for the computation of electromagnetic forces in continuous medium," *Int. Compumag Society Newsletter*, vol. 11, no. 2, pp. 3–9, 2004.

[12] I. Coenen, M. Herranz Gracia, and K. Hameyer, "Influence and evaluation of non-ideal manufacturing process on the cogging torque of a permanent magnet excited synchronous machine," in *XXIth Symp. Electromagnetic Phenomena in Nonlinear Circuits (EPNC)*, Essen, Germany, Jun. 2009.